

Supplementary Figure II. Cellular distribution of NP in ischemic muscles.

A, Representative light (upper panels) and fluorescent (lower panels) stereomicrographs of the gastrocnemius muscles isolated from a control, non-ischemic hindlimb and those from an ischemic hindlimb injected with FITC-NP or FITC alone. B, Quantitative analysis of the magnitude of intracellular FITC fluorescence signals in the gastrocnemius muscles are shown. The data were compared using two-way ANOVA followed by Bonferroni's multiple comparison tests. * $p < 0.05$ versus control condition. † $p < 0.05$ versus FITC. C, Immunofluorescent staining of cross-sections from ischemic muscle 3 days after a FITC-NP or FITC only injection stained with the endothelial marker CD31 (red). Scale bars: 100 μm .

Supplemental Table I. Serum concentration of glucose, triglyceride and insulin at 3

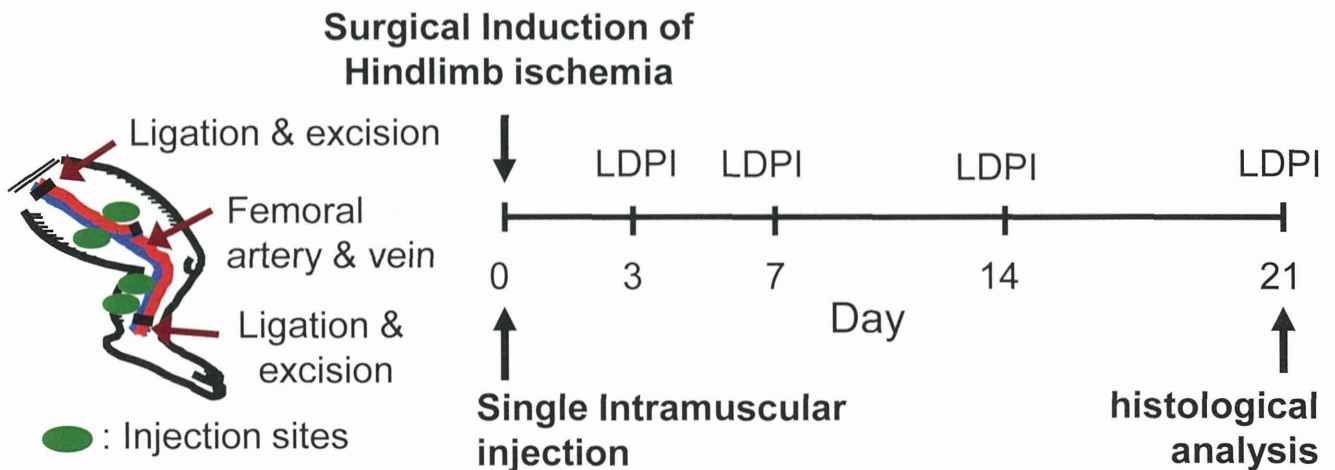
weeks after daily oral administration of pioglitazone

Oral Pioglitazone (mg/kg/day)	Body Weight (g)	Serum Glucose (mg/dL)	Serum Triglyceride (mg/dL)	Serum Insulin (μ IU/mL)
0	24.4 \pm 0.6	303 \pm 33	39 \pm 2	ND
1	24.5 \pm 1.0	272 \pm 23	55 \pm 11	ND
500	24.4 \pm 1.2	309 \pm 114	60 \pm 12	ND
1000	23.6 \pm 0.9	280 \pm 48	63 \pm 10	ND

ND: not detected (<0.3 μ IU/mL)

The data are shown as the mean \pm SEM (n=2-5 each).

Supplementary Figure I Nagahama R *et al.*



Protocol 1.

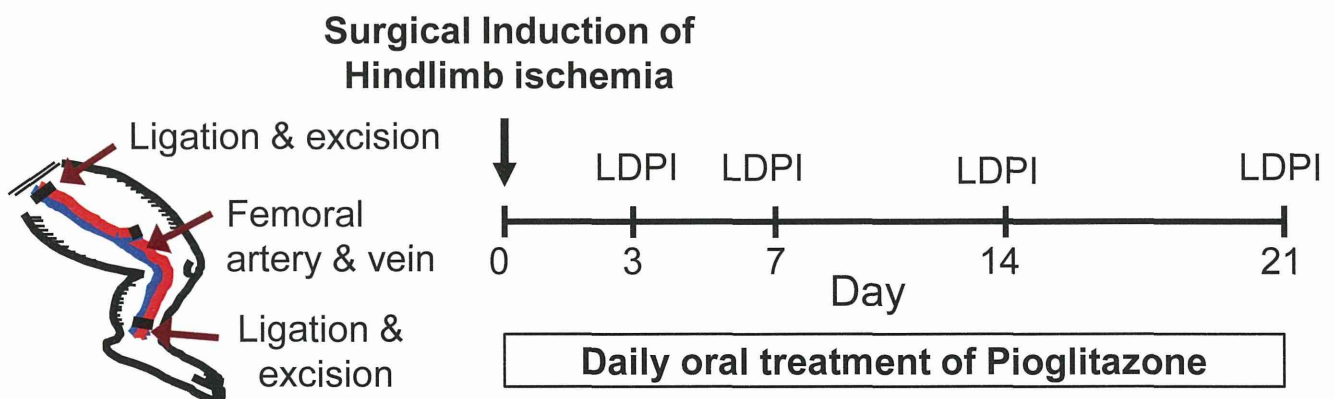
- vehicle
- FITC-NP (control NP)
- Pioglitazone (0.1, 1 $\mu\text{g}/\text{kg}$)
- Pio-NP (0.1, 1 $\mu\text{g}/\text{kg}$ as Pioglitazone)

Protocol 2.

- vehicle
- Pio-NP (1 $\mu\text{g}/\text{kg}$ as Pioglitazone)
- GW9662 i.p. + Pio-NP (1 $\mu\text{g}/\text{kg}$ as Pioglitazone)

Protocol 3.

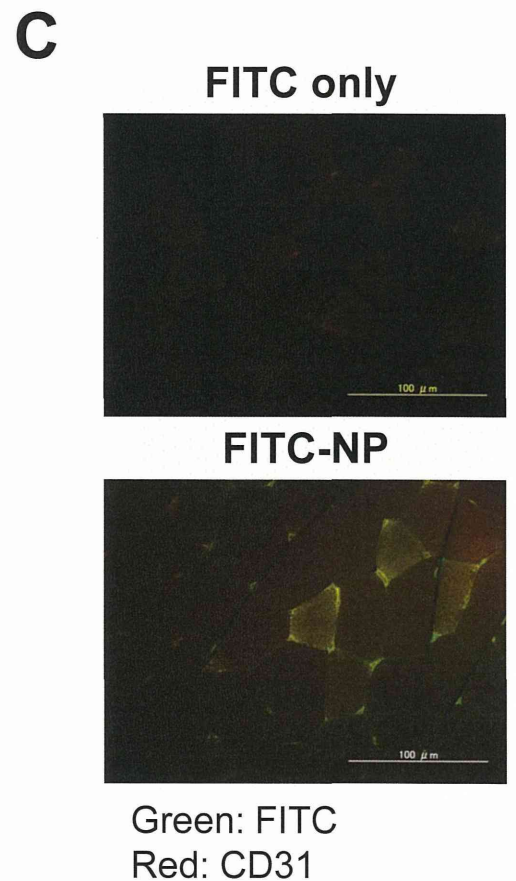
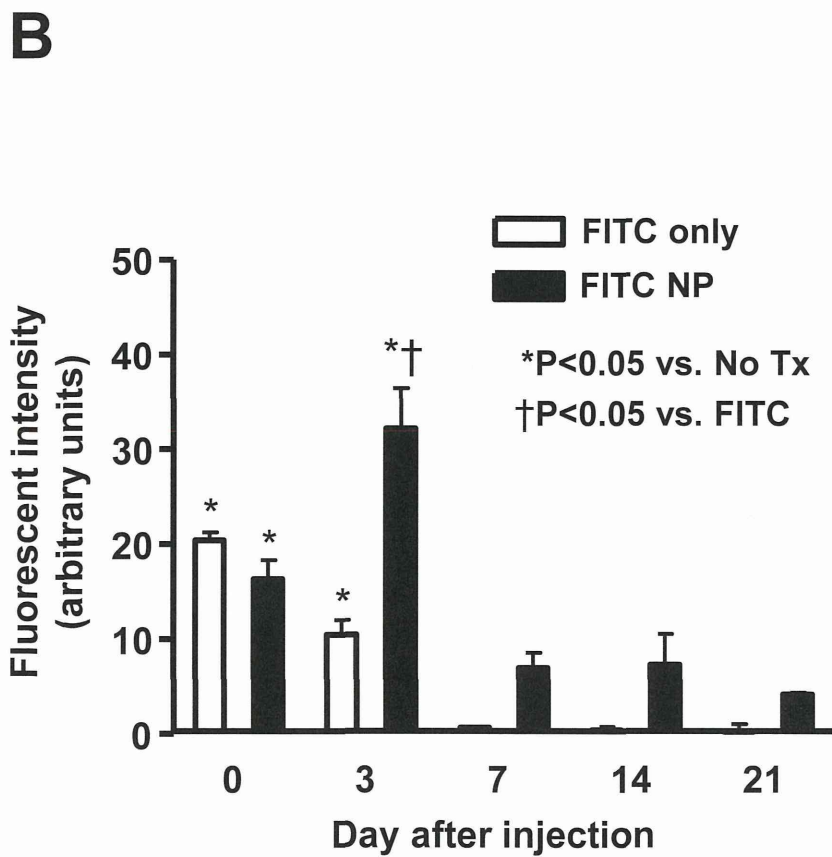
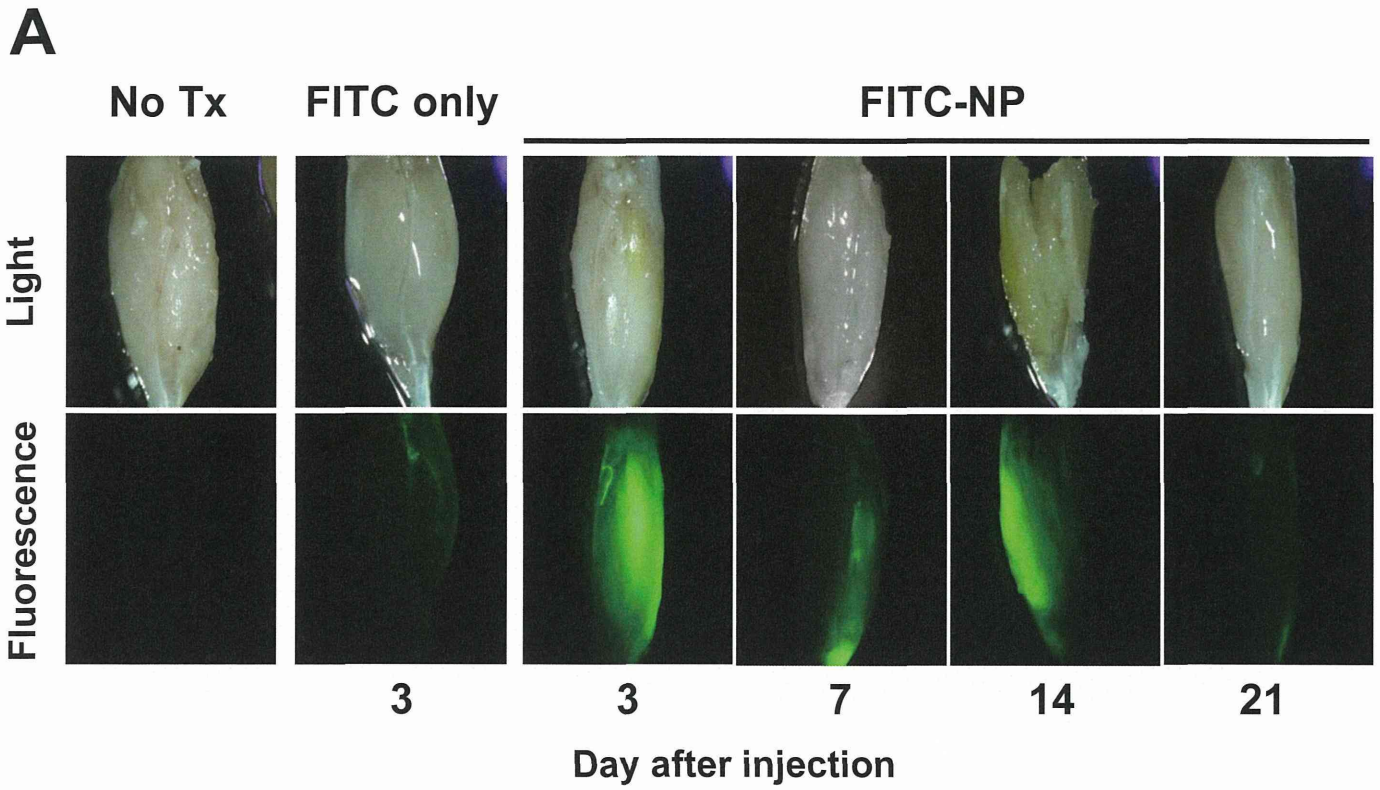
- WT mice, vehicle
- WT mice, Pio-NP (1 $\mu\text{g}/\text{kg}$ as Pioglitazone)
- eNOS^{-/-} mice, vehicle
- eNOS^{-/-} mice, Pio-NP (1 $\mu\text{g}/\text{kg}$ as Pioglitazone)



Protocol 4.

- Vehicle
- Pioglitazone (1, 500, 1000 $\mu\text{g}/\text{kg}$)

Supplementary Figure II Nagahama R *et al.*



Original Article

Pitavastatin-Incorporated Nanoparticle-Eluting Stents Attenuate In-Stent Stenosis without Delayed Endothelial Healing Effects in a Porcine Coronary Artery Model

Noriaki Tsukie¹, Kaku Nakano¹, Tetsuya Matoba¹, Seigo Masuda¹, Eiko Iwata¹, Miho Miyagawa¹, Gang Zhao³, Wei Meng³, Junji Kishimoto², Kenji Sunagawa¹ and Kensuke Egashira¹

¹Department of Cardiovascular Medicine, Graduate School of Medical Sciences, Kyushu University, Fukuoka, Japan

²Digital Medicine Initiative, Graduate School of Medical Sciences, Kyushu University, Fukuoka, Japan

³Department of Cardiovascular Medicine, 6th People's Hospital, Shanghai Jiatong University, Shanghai, China

Aim: The use of currently marketed drug-eluting stents presents safety concerns including increased late thrombosis, which is thought to result mainly from delayed endothelial healing effects (impaired re-endothelialization resulting in abnormal inflammation and fibrin deposition). We recently developed a bioabsorbable polymeric nanoparticle (NP)-eluting stent using a novel cationic electrodeposition technology. Statins are known to inhibit the proliferation of vascular smooth muscle cells (VSMC) and to promote vascular healing. We therefore hypothesized that statin-incorporated NP-eluting stents would attenuate in-stent stenosis without delayed endothelial healing effects.

Methods: Among six marketed statins, pitavastatin (Pitava) was found to have the most potent effects on VSMC proliferation and endothelial regeneration *in vitro*. We thus formulated a Pitava-NP-eluting stent (20 µg Pitava per stent).

Results: In a pig coronary artery model, Pitava-NP-eluting stents attenuated in-stent stenosis as effectively as polymer-coated sirolimus-eluting stents (SES). At SES sites, delayed endothelial healing effects were noted, whereas no such effects were observed in Pitava-NP-eluting stent sites.

Conclusion: Pitava-NP-eluting stents attenuated in-stent stenosis as effectively as SES without the delayed endothelial healing effects of SES in a porcine coronary artery model. This nanotechnology platform could be developed into a safer and more effective device in the future.

J Atheroscler Thromb, 2013; 20:32-45.

Key words; Statin, Nanotechnology, Drug delivery system, Signal transduction

Introduction

Increased risk of late in-stent thrombosis resulting in acute coronary syndrome (unstable angina, acute myocardial infarction and death) after the use of drug-eluting stent (DES) devices has become a major safety concern¹⁻³. These adverse effects are thought to result mainly from the anti-healing effects of the drugs (sirolimus and paclitaxel) on endothelial cells, leading

to impaired re-endothelialization, excessive inflammation, proliferation and fibrin deposition⁴⁻⁶. These "anti-healing" drugs are used in most newer generation DESs, leading to continued safety concerns; therefore, the cellular and/or molecular targeting of both VSMC proliferation and re-endothelialization is an essential requirement for the development of more efficient and safer DESs. The use of an anti-healing approach that accelerates re-endothelialization, protects against thrombosis and decreases restenosis is warranted. Comparator analysis of endothelial cell coverage in four marketed polymeric DESs in rabbits has demonstrated a disparity in arterial healing; notably, all DESs examined showed a lack of endothelial anticoagulant function, independent of endothelial coverage⁷.

Address for correspondence: Kensuke Egashira, Department of Cardiovascular Medicine, Graduate School of Medical Science, Kyushu University, 3-1-1, Maidashi, Higashi-ku, Fukuoka 812-8582, Japan

E-mail: egashira@cardiol.med.kyushu-u.ac.jp

Received: March 18, 2012

Accepted for publication: June 21, 2012

We hypothesized that HMG-CoA reductase inhibitors, so-called statins, are appropriate candidate drugs for the anti-healing strategy because the vascular endothelium is a major target for the pleiotropic (non-LDL-related) vasculoprotective effects of statins⁸. In cell culture experiments *in vitro*, statins reportedly promoted endothelial regeneration and inhibited VSMC proliferation and tissue factor expression^{8, 9}. Systemic administration of statins has been reported to inhibit balloon injury-induced and in-stent neointima formation in non-hypercholesterolemic animals. Most of these beneficial effects of statins on neointima formation in animals, however, were observed following daily administration of high doses^{8, 10} (rosuvastatin 20 mg/kg per day¹¹), pitavastatin 40 mg/kg per day¹²), simvastatin 40 mg/kg per day¹³); this may lead to serious adverse side effects in a clinical setting. Furthermore, it has been reported that the use of polymer-coated stents with atorvastatin or cerivastatin has no consistent effect on neointima formation in a porcine in-stent stenosis model^{14, 15}. Randomized clinical studies in humans have reported no definite effects of statins within the clinical dose range with respect to indices of restenosis after coronary balloon angioplasty¹⁶⁻¹⁹ or coronary stenting^{20, 21}); therefore, preventing in-stent restenosis via statin-mediated “anti-healing” effects requires an efficient local drug delivery system.

To overcome this problem, we recently introduced nanoparticles (NP) formulated from the bioabsorbable polymer poly(DL-lactide-co-glycolide) (PLGA) and succeeded in formulating an NP-eluting stent by a cationic electrodeposition coating technology²²). Therefore, we hypothesized that statin-NP-eluting stents could be an innovative therapeutic “anti-healing” strategy for treating in-stent stenosis *in vivo*.

Materials and Methods

Statins (simvastatin, pitavastatin, atorvastatin, rosuvastatin, fluvastatin, and pravastatin) were purchased, extracted from products, and purified.

Human Coronary Artery Smooth Muscle Cell Proliferation

Human coronary artery smooth muscle cells (SMC) were cultured as previously described^{22, 23} and plated into 96-well culture plates at 1×10^4 cells per well in SMGM2. Proliferation was stimulated by adding human PDGF at 10 ng/mL (Sigma, Tokyo, Japan) or 10% FBS to each well. Either vehicle alone or several concentrations of statins, sirolimus, or paclitaxel were added to the well. Cellular proliferation responses

were determined by evaluating the 5'-bromo-2'-deoxyuridine (BrdU) incorporation rate and/or by a cell counting method, as previously described^{22, 23}.

Human Endothelial Cell Scratch Motility Assay

A scratch motility assay using human umbilical vein endothelial cells (HUVEC) was performed to assess the re-endothelialization response following endothelial denudation. HUVECs were seeded in collagen I-coated 24-well plates at a density of 2×10^4 cells per well and grown to confluence with EGM2. The monolayers were wounded with a pipet tip, washed with PBS twice, photographed and incubated at 37°C with EBM containing 0.5% BSA containing VEGF₁₆₅ (10 ng/mL, R & D) in the presence or absence of statins, sirolimus, or paclitaxel. After five hours, cells were photographed, and the number of cells that had migrated into the wounded area was counted.

Western Blot Analysis

Human aortic endothelial cells (HAEC) were cultured to confluence in 3 cm dishes and rendered quiescent for 24 hours before stimulation with 1 U/mL thrombin (Sigma). Sirolimus, paclitaxel (both Sigma), and pitavastatin were added to the cells one hour before thrombin (1 U/mL) stimulation. Tissue factor protein expression was determined by Western blot analysis. In another set of experiments, sirolimus was added to HAEC and effects of pitavastatin on sirolimus-induced changes in endothelial nitric oxide synthase (eNOS) and protein kinase B (Akt) protein were examined.

Cell extracts (20 μ g) were resolved on 10% reducing SDS-PAGE gels and blotted onto nitrocellulose membranes (Bio-Rad, Hercules, CA). Antibodies against human tissue factor (Calbiochem), phosphorylated-Akt (ser473), phosphorylated-eNOS (ser1177), Akt (Cell Signaling), eNOS (Affinity BioReagents) were used. Immune complexes were visualized with horseradish peroxidase-conjugated secondary antibodies (Pierce, Rockford, IL) using the ECL Plus system (Amersham Biosciences) and were detected with the ECL Detection Kit (Amersham). Blots were normalized against GAPDH expression (Sigma).

Preparation of Cationic PLGA Nanoparticles (NP) with Surface Modification with Chitosan

A lactide/glycolide copolymer (PLGA) with an average molecular weight of 20,000 and a lactide to glycolide copolymer ratio of 75:25 (PLGA7520; Wako Pure Chemical Industries, Osaka, Japan) was used as wall material for the NPs because the bioabsorption

half-life of this product is two weeks in rat tissue (manufacturer's instructions). PLGA NPs incorporated with the fluorescent marker fluorescein isothiocyanate (FITC; Dojindo laboratories, Kumamoto, Japan) or with pitavastatin were prepared by a previously reported emulsion solvent diffusion method in purified water²². FITC- and pitavastatin-loaded PLGA NPs contained 5.0% (w/v) FITC and 6.5% (w/v) pitavastatin, respectively, and were preserved as freeze-dried material. The mean particle size was analyzed by the light scattering method (Microtrack UPA150; Nikkiso, Tokyo, Japan). The average diameter of the PLGA NPs was 226 ± 29 nm. The surface charge (zeta potential) was also analyzed by Zetasizer Nano (Sysmex, Hyogo, Japan) and was found to be cationic (+36 mV at pH 4.4).

Preparation of NP-Eluting Stents by Cationic Electrodeposition Coating Technology

The 15 mm-long stainless-steel, balloon-expandable stents (Multilink) were ultrasonically cleaned in acetone, ethanol, and demineralized water. The cationic electrodeposited coating was prepared on cathodic stents in NP solution at a concentration of 5 g/L in distilled water with a current maintained between 2.0 and 10.0 mA by a direct current power supply (DC power supply; Nippon Stabilizer Co, Tokyo, Japan) for different periods under sterile conditions.^{28, 31} The coated stents were then rinsed with demineralized water and dried under a vacuum overnight. This electrodeposition coating procedure produced a coating of approximately 367 ± 77 μg of the PLGA NPs per stent and 20 ± 4 μg of pitavastatin per stent ($n=12$). The surfaces of some NP-coating stents were examined with scanning electron microscopy (JXM8600; JEOL, Tokyo, Japan), and it was confirmed that the NPs were structurally intact and cohesive²².

Analysis of Endothelial Surface Coverage by en Face Scanning Electron Microscopy

For evaluation of endothelial coverage, stents were excised seven days after implantation. The stented arteries were fixed *in situ* with 10% neutral-buffered formalin after perfusion with lactated Ringer's solution to remove blood. The samples were further fixed by immersion and then bisected longitudinally with one half processed for scanning electron microscopy (SEM).

Composites of serial en face SEM images acquired at low power ($\times 15$ magnification) were digitally assembled to provide a complete view of the entire luminal stent surface. The images were further enlarged ($\times 200$

magnification), allowing direct visualization of endothelial cells. The extent of endothelial surface coverage above and between stent struts was traced and measured by morphometry software. The results are expressed as a percentage of the total surface area above or between struts or the total and percentage area lacking coverage at each repeated crown along the longitudinal axis from the proximal to the distal orientation. Endothelial cells were identified as sheets of spindle- or polygonal-shaped monolayers in close apposition, a distinguishing feature from other cell types in en face preparations²⁴. By contrast, intimal smooth muscle cells showed elongated processes and were generally stacked in disorganized or haphazard layers²⁴. Other adherent cells present on stent surfaces included platelets, characteristically 1 to 2 μm in size with an irregular discoid appearance, and inflammatory cells, which were round and varied from 7 to 10 μm in diameter with a ruffled surface. Struts uncovered by endothelium were completely bare or contained thrombi consisting of focal platelet and fibrin aggregates intermixed with red blood cells and inflammatory cells.

Measurements of Pitavastatin Concentration in Serum and Arterial Tissue

Concentrations of pitavastatin in serum and stented arterial tissue were measured at predetermined time points using a column-switching high performance liquid chromatography (HPLC) system as previously reported²⁵. Briefly, the column-switching HPLC system consists of two LC-10AD pumps, a SIL-10A auto-sampler, a CTO-10A column oven, a six-port column-switching valve, and an SPD-10A UV-detector (all from Shimadzu, Kyoto, Japan). The column temperature was maintained at 40°C. Pre-prepared serum or tissue homogenate sample solutions were injected from the auto-sampler into the HPLC system, and statin in the sample solutions was detected at 250 nm with a UV detector. The detected peak area was measured with Lc solution software (Shimadzu, Kyoto, Japan).

Animal Preparation and Stent Implantation

All *in vivo* experiments were reviewed and approved by the Committee on Ethics in Animal Experiments, Kyushu University Faculty of Medicine, according to the Guidelines of the American Physiological Society.

Domestic male pigs (Kyudo, Tosu, Japan; aged 2 to 3 months and weighing 25 to 30 kg) received orally aspirin (330 mg/day) and ticlopidine (200 mg/day) until euthanasia from 3 days before stent implantation

Table 1. Inhibitory effects of 6 commercially available statins on proliferation of human coronary artery smooth muscle cells

	IC ₅₀ values (nmol/L)	efficacy ratio	95% Wald confidence intervals	<i>p</i> value
pitavastatin	193	1	–	–
fluvastatin	836	0.230	0.119, 0.446	<0.001
atorvastatin	2512	0.077	0.039, 0.150	<0.001
simvastatin	3951	0.049	0.023, 0.104	<0.001
rosuvastatin	Not calculated	Not calculated	Not calculated	Not calculated
pravastatin	Not calculated	Not calculated	Not calculated	Not calculated

n = 6 each. *p* values versus pitavastatin by Wald tests in 4-parameter logistic regression model.

procedure. Animals were anesthetized with ketamine hydrochloride (15 mg/kg, IM) and pentobarbital (20 mg/kg, IV). They were then intubated and mechanically ventilated with room air. A preshaped Judkins catheter was inserted into the carotid artery and advanced into the orifice of the left coronary artery. After systemic heparinization (100 IU/kg) and intracoronary administration of nitroglycerin, coronary angiography of the left coronary artery was performed with the use of contrast media (iopamidol 370) in a left oblique view with the angiography system (Toshiba Medical, Tokyo, Japan).

Animals were divided into groups, which underwent deployment of either non-coated bare metal stents (1 week: *n* = 3, 4 weeks: *n* = 12), FITC-incorporated NP-eluting stents (4 weeks: *n* = 12), pitavastatin-incorporated NP-eluting stents (1 week: *n* = 3, 4 weeks: *n* = 12), or sirolimus-eluting stents (Cypher; 3 mm × 15 mm) (1 week: *n* = 3, 4 weeks: *n* = 12) in the left anterior descending (LAD) or the left circumflex (LCx) coronary arteries. After arterial blood samples were taken, animals were given a lethal dose of anesthesia after 1 or 4 weeks, and the stented arterial sites and contralateral non-stented sites were excised for biochemical, immunohistochemical, and morphometric analyses.

As another set of experiments, animals were treated with intracoronary administration of pitavastatin-NP at 300 μg (a similar dose to that coated on pitavastatin-NP eluting stent, 4 weeks: *n* = 6) and 3000 μg (10x dose coated on pitavastatin-NP eluting stent, 4 weeks: *n* = 6) containing 20 and 200 μg pitavastatin, respectively, immediately after deployment of bare metal stents. Pitavastatin-NPs were diluted with 10 mL saline. Intracoronary administration of 10 mL saline was used as a control experiment (4 weeks: *n* = 5).

A segment with a mean coronary diameter of 2.5 mm was selected by using quantitative coronary angiography with a stent-to-artery ratio of approximately

1.1 : 1.2. A balloon catheter mounted with a stent was then advanced to the pre-selected coronary segments for deployment over a standard guide-wire. The balloon catheter was inflated at 15 atm for 60 seconds once and was then slowly withdrawn, leaving the stent in place.

Quantitative coronary angiography (Toshiba Medical, Tokyo, Japan) was performed before, immediately after, and 4 weeks after stent implantation to examine the coronary arterial diameter at stented and non-stented sites. The image of a Judkins catheter was used as reference diameter. Arterial pressure, heart rate, and ECG were continuously monitored and recorded on a recorder.

Histopathological Study

Four weeks after the coronary angiographic study, animals were euthanized with a lethal dose of sodium pentobarbital (40 mg/kg intravenously), and histological analysis was performed. The left coronary artery was perfused with 10% buffered formalin at 120 mmHg and fixed for 24 hours. The stented artery segments were isolated and processed as described previously²⁶. The segment was divided into two parts at the center of the stent and then embedded in methyl methacrylate mixed with n-butyl methacrylate to allow for sectioning through the metal stent struts. Serial sections were stained with elastic van Gieson and hematoxylin-eosin (HE). The neointimal area, the area within the internal elastic lamina (IEL), and the lumen area were measured by computerized morphometry, which was carried out by a single observer who was blinded to the experimental protocol. All images were captured by an Olympus microscope equipped with a digital camera (HC-2500) and were analyzed using Adobe Photoshop 6.0 and Scion Image 1.62 software. The injury, inflammation, fibrin, hemorrhage and re-endothelialization scores were determined at each strut site, and mean values were calculated for each stented segment.

Statistical Analysis

Data are expressed as the means \pm SE. Statistical analysis of differences between two groups was performed with the unpaired *t*-test, and differences among groups were analyzed using ANOVA and multiple comparison tests.

Efficacy ratios (IC_{50} values) of the statins were tested using Wald tests in a four-parameter logistic regression model. Point estimates and Wald 95% confidence intervals for efficacy ratios were calculated. Statistical calculations were performed with SAS pre-clinical package software version 9.1.3 (SAS Institute Inc., Japan, Tokyo). *P* values < 0.05 were considered significant.

Results

Effects of Statins on Human Coronary Artery Smooth Muscle Cell Proliferation and Endothelial Cell Scratch Motility Assay

To incorporate statins into the NP-eluting stent design, the effects of statins were compared. In the human CASMC proliferation assay (% inhibition of BrdU index), hydrophilic statins (rosuvastatin and pravastatin) had no effects on PDGF-induced proliferation; thus, calculation of the IC_{50} value was impossible for those statins (Table 1). By contrast, the other four statins showed concentration-dependent inhibition. The IC_{50} values of the four statins are shown in Table 1, which indicates that the value for pitavastatin is lowest.

In the human endothelial cell scratch motility assay (re-endothelialization *in vitro*), only pitavastatin increased the re-endothelialization response following scratch injury; the other five statins showed no such effects (Fig. 1). In addition, there was no difference in the re-endothelialization response among the five statins.

Effects of Pitavastatin, Sirolimus, and Paclitaxel on Human Coronary Artery Smooth Muscle Cell Proliferation, Endothelial Cell Scratch Motility Assay, and Tissue Factor Expression in Human Endothelial Cells

To incorporate pitavastatin into the NP-eluting stent design, the effects of pitavastatin were then compared with those of sirolimus and paclitaxel. All three drugs inhibited human CASMC proliferation (Fig. 2). In the human endothelial cell scratch motility assay, sirolimus did not affect the re-endothelialization response, whereas the response was significantly delayed in paclitaxel-treated endothelial cells (Fig. 1).

Because tissue factor has a primary role in stent

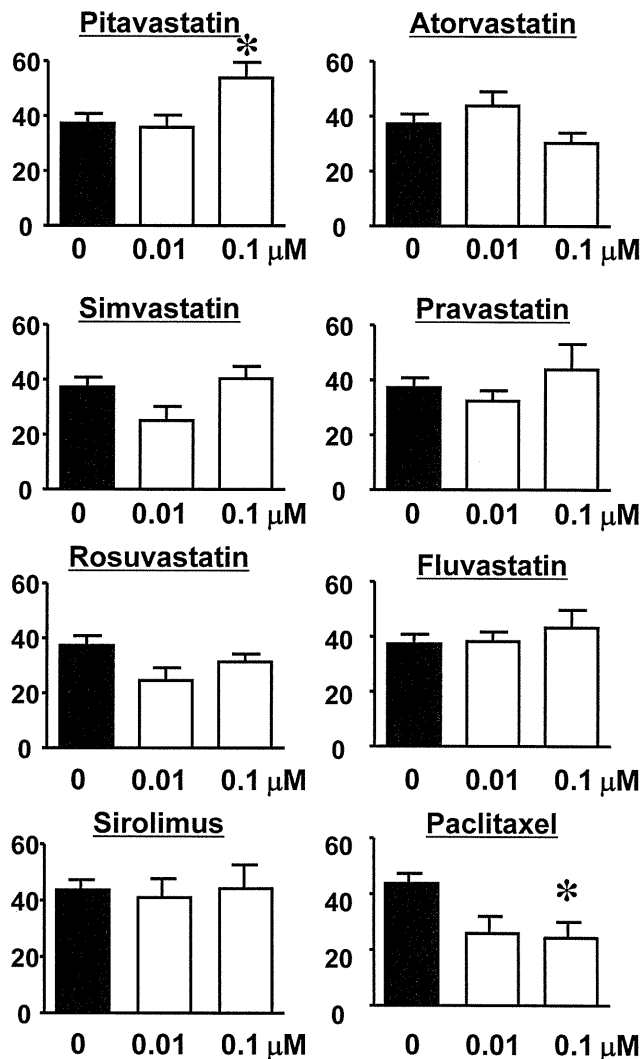


Fig. 1. Human umbilical vein endothelial cell scratch motility assay *in vitro*. Vertical axis denotes the number of migrated cells into the scratched area. **p* < 0.05 vs no treatment by one-way ANOVA followed with Dunnett's multiple comparison test (*n* = 6-8 each).

thrombosis, its protein expression was examined in human endothelial cells. As previously reported by others²⁷), both sirolimus and paclitaxel enhanced the thrombin-induced tissue factor expression (Fig. 2). By contrast, pitavastatin inhibited tissue factor expression (Fig. 2).

Effects of Pitavastatin on Sirolimus-Induced Down Regulation of eNOS in Human Endothelial Cells

Sirolimus down regulated phosphorylated-eNOS and decreased phosphorylated Akt (a representative down stream signal of eNOS), while sirolimus had no effects on eNOS and Akt protein expression (Fig. 3).

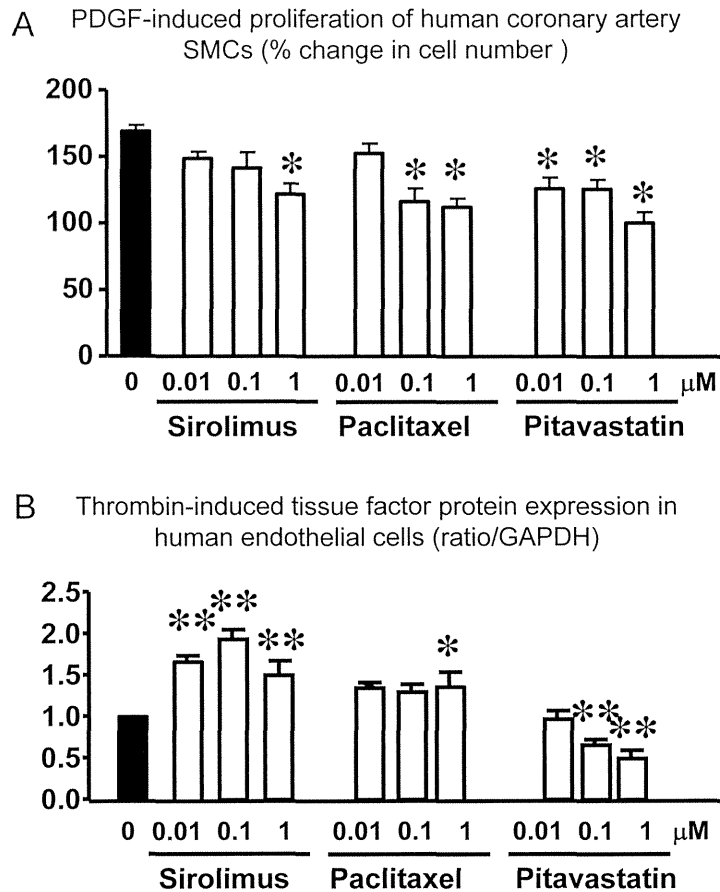


Fig. 2. Effects of pitavastatin, sirolimus, and paclitaxel on human CASMC proliferation and human AEC tissue factor expression.

A, PDGF-induced proliferation (% increase in cell number) of human CASMCs. Data are the mean ± SEM (*n*=6 each). **p*<0.01 versus control by one-way ANOVA followed with Dunnett’s multiple comparison test. B, Thrombin-induced tissue factor protein expression in human AECs. Data are the mean ± SEM (*n*=6 each). **p*<0.01 versus thrombin alone by one-way ANOVA followed with Dunnett’s multiple comparison test.

Pitavastatin nearly normalized the sirolimus-induced decrease in p-eNOS and p-Akt protein expression.

Effects of Pitavastatin and Pitavastatin-NP on Human CASMC Proliferation

Both pitavastatin and pitavastatin-NP inhibited the FBS-induced proliferation of human CASMC. The inhibitory activities of pitavastatin-NP were greater than those of 0.01, 0.1, and 1 μM pitavastatin only (Fig. 4).

Effects of Pitavastatin-NP-Eluting Stents and Sirolimus-Eluting Stents on Neointima Formation Four Weeks after Stent Implantation

Two animals in the control bare metal stent

group died suddenly between weeks three and four; therefore, these animals were excluded from angiographic and histopathological analyses, which were performed in 34 pigs (10 in the control bare metal stent group, 12 in the FITC-NP-eluting stent group, 12 in the pitavastatin-NP eluting stent group, and 12 in the sirolimus-eluting stent group).

Quantitative coronary arteriography revealed that (1) there was no significant difference in the coronary diameter before and immediately after stent implantation or in the stent-to-artery ratio among the four groups and (2) the coronary diameter was less in the control bare metal and the FITC-NP-eluting stent sites than in the pitavastatin-NP-eluting stent and sirolimus-eluting stent sites four weeks after stenting